

Synthesis, Characterization and Quantum Chemical Computational Studies on the N,N'-Dibenzylidene-3,3'-dimethoxybenzidine

Lalehan AKYÜZ^{1*} 

¹ Aksaray University, Technical Vocational School, Department of Chemistry Technology, 68100, Aksaray, Turkey

Geliş / Received: 01/05/2019, Kabul / Accepted: 30/05/2020

Abstract

In the present study, the thermally stable N,N'-Dibenzylidene-3,3'-dimethoxybenzidine was synthesized by the condensation reaction between o-dianisidine and benzaldehyde. Elemental analysis, FT-IR, H-NMR, TGA, XRD and SEM was used to characterization of synthesized compound. In addition to the synthesis, the quantum chemical calculations of the synthesized molecule were performed using DFT method, B3LYP, in 6-31G** basis set in the ground state. Experimental and calculated results were compared with each other. The calculated chemical shifts and vibrational wavenumbers were in compromise with the experimental values. In addition, the solvent effects were investigated for the Mulliken charges and thermodynamic properties. The molecular electrostatic potential map, frontier molecular orbitals, QSAR parameters, and geometrical properties were obtained theoretically.

Keywords: N,N'-Dibenzylidene-3,3'-dimethoxybenzidine, Synthesis, Characterization, DFT study

N, N'-Dibenziliden-3,3'-dimetoksibenzidinin Sentezi, Karakterizasyonu ve Kuantum Kimyasal Hesaplama Çalışmaları

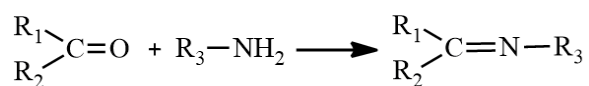
Öz

Bu çalışmada, termal olarak kararlı N, N'-Dibenziliden-3,3'-dimetoksibenzidin bileşiği, o-dianisidin ve benzaldehit arasındaki kondenzasyon reaksiyonu ile sentezlenmiştir. Sentezlenen bileşiğin karakterizasyonunda element analizi, FT-IR, H-NMR, TGA, XRD ve SEM kullanılmıştır. Senteze ek olarak, sentezlenen molekülün kuantum kimyasal hesaplamaları, DFT metodu ile temel durumda B3LYP/6-31G ** temel seti ile yapılmıştır. Deneysel ve hesaplanan sonuçlar birbirleriyle karşılaştırılmıştır. Hesaplanan kimyasal kaymalar ve titreşim dalgalanmaları deneysel değerlerle uyumaktadır. Ek olarak, Mulliken yüklerini ve termodinamik özelliklere çözücü etkileri araştırılmıştır. Moleküler elektrostatik potansiyel haritası, sınır moleküler orbitaller, QSAR parametreleri ve geometrik özellikler teorik olarak elde edilmiştir.

Anahtar Kelimeler: N,N'-Dibenziliden-3,3'-dimetoksibenzidin, Sentez, Karakterizasyon, DFT Metod.

1. Introduction

Acid catalysed condensation reaction of carbonyl compounds with primary amines have been formed the Schiff bases containing azomethine groups ($-C=N-$). Schiff bases have been used in many different application areas such as polymer stabilizers, catalysts, pigments and dyes (Gupta, Sutar, & Lin, 2009; Gümrükçü, Karaoğlan, Erdoğan, Gül, & Avcıata, 2012; Lorcy, Bellec, Fourmigué, & Avarvari, 2009). Also, Schiff bases have been used in medicinal and pharmaceutical fields, because of their biological activities such as antibacterial, anti-proliferative, antiviral, antipyretic and anti-inflammatory properties (Ebrahimi, Hadi, & Al-Ansari, 2013; Przybylski, Huczynski, Pyta, Brzezinski, & Bartl, 2009). The classical condensation reaction of monosubstitue compounds including carbonyl and primer amines occurs a Schiff base with high yields. The general mechanism of the reaction was given in Scheme 1. All steps in this reaction are reversible and thermodynamically controlled conditions. Similarly, benzidine derivatives contain two primer amines groups can be used in order to obtain new Schiff bases. Benzidine derivatives have been of great interest due to the usage of the in many different application areas such as sensor materials, the building blocks in the synthesis of new organic compounds and in cell biology.



Scheme 1. The general reaction mechanism of formation of Schiff bases

Im et al. (2018) synthesized a benzidine derivative as a diamine compound, using o-dianisidine and benzaldehyde. In this study, the crystallographic structure was reported by

the authors. Also, Kaya et al. (2009) synthesized four Schiff Base derivatives by reaction of o-dianisidine with vanillin, salicylaldehyde, 3-ethoxy-4-hydroxybenzaldehyde and 4-hydroxybenzaldehyde in order to synthesize new polymers. The authors prepared the new polymers using synthesized monomers and investigated the thermal, optical and electrical properties of the polymers.

In the current study, a new thermally stable Schiff base was synthesized by the condensation reaction between o-dianisidine and benzaldehyde. Elemental analysis, FT-IR, 1H -NMR, TGA, XRD and SEM analyses were used for characterization of the obtained compound. Also, the theoretical calculations of the synthesized compound were performed via density functional theory (DFT) method, B3LYP in 6-31G** basis set by using SPARTAN' 16 for Windows software. The electronic properties of the title compound such as frontier molecular orbital energies and Mulliken atomic charges and spectroscopic properties such as FT-IR, 1H NMR and QSAR parameters (Karelson, Lobanov & Katritzky, 1996) were calculated, in order to compare the experimental and theoretical results. Obtained results were discussed.

2. Experimental Section

2.1. Materials and instrumentation

All of the chemicals used in the experiments were purchased from Sigma-Aldrich. The chemicals and solvents were of extra-pure grade and used as received without further purification. FT-IR spectra of obtained samples were recorded on a Perkin-Elmer FT-IR spectrometry at 4000-650 cm^{-1} . Thermal stability of samples was obtained with Perkin Elmer Diamond Thermogravimetric Analyser under nitrogen atmosphere with a heating rate

10 C°. XRD analysis was performed using on a Bruker D8 Advance instrument with Cu K α line focused radiation at 40 kV and 40 mA from $2\theta = 3.0^\circ$ up to 90° . SEM images of samples were taken on a LEICA/CAMBRIDGE LEO S-440 STEREOSCAN.

2.2. Synthesis of N,N'-dibenzylidene-3,3'-dimethoxybenzidine

3,3'-dimethoxybiphenyl-4,4'-diamine (0.5 g, 0.0020 mol) and benzaldehyde (0.26 g, 0.0041 mol) were added 5 mL THF; the mixture was refluxed for 5 hours at 65°C . The completion of the reaction was intermittently checked by TLC technique. Then the mixture was cooled down to room temperature. The precipitate was filtered off and washed with petroleum ether. Obtained brown solid was dried at under the vacuum at 50°C . Yield: Elemental Analysis: Calculated; (C₂₃H₁₅N₂O₂)_n: C 78.60; H 4.27; N 7.98; O 9.12. Found; C76.34; H4.61; N14.20.

3. Computational Procedure

In recent years, quantum mechanical methods have become important in order to predict of molecular properties due to its accurate and accordance with experimental data. DFT has been extensively used method among the quantum mechanical methods because of its reliable results (Bachrach, 2008). In this study, the molecular structure of the synthesized compound was optimized by DFT method B3LYP in 6-31G** basis set in gas phase. The SPARTAN'16 software package (Spartan 18 for Windows) was employed to perform optimization of the synthesized compound in the ground state. Vibrational frequencies of the optimized molecular structure were computed at the same levels of

theory. The GIAO method was used to calculate the ¹H NMR chemical shifts. HOMO-LUMO energies, atomic charges, bond orders, bond lengths, bond angles, dihedral angles were calculated as electronic parameters. Also, the heat of formation and QSAR parameters were obtained and the results discussed.

4. Results and Discussion

4.1. Experimental results

4.1.1. FT-IR Analysis

The FT-IR analysis was performed to investigate the molecular structure and functional groups of the title compound. The FT-IR spectra of the studied compound and o-dianisidine were given in Fig. 1. As seen from the Fig. 1, the peaks at 3017 cm^{-1} correspond to the aromatic C–H vibrations. 2962 and 2925 cm^{-1} are due to the aliphatic C–H vibrations. While strong band at 1626 cm^{-1} corresponds to the characteristic band of the CH=N group of Schiff bases. Also, when the spectrum of synthesized compound is compared to that of the starting material of 3,3'-dimethoxybiphenyl-4,4'-diamine spectrum, i) –NH₂ stretching vibrations at 3411 and 3343 cm^{-1} were disappeared, ii) –N–H scissoring vibration of primer amine at 1617 cm^{-1} was disappeared, iii) C–O–C stretching at 1224 cm^{-1} was shifted to 1247 cm^{-1} . All of these findings prove that the new compound was successfully synthesized.

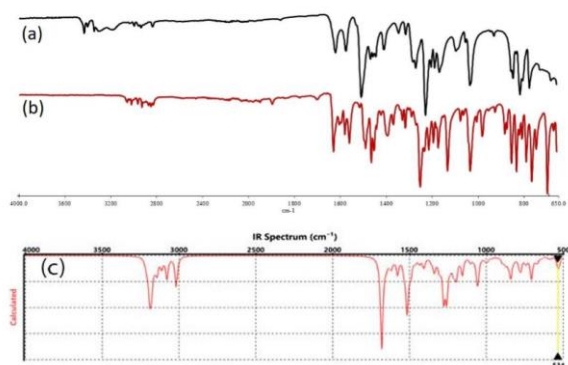


Fig. 1 Comparison of experimental infrared spectra of *o*-dianisidine (a), N,N'-Dibenzylidene-3,3'-dimethoxybenzidine (b) and simulated infrared spectrum of N,N'-Dibenzylidene-3,3'-dimethoxybenzidine (c).

4.1.2. NMR Spectra

The ^1H NMR spectrum given in the Fig 2a. of the N,N'-Dibenzylidene-3,3'-dimethoxybenzidine was recorded in *d*₆-dimethylsulfoxide (DMSO) as a solvent and chemical shift values given in Table 2. It was found that the ^1H NMR spectrum of synthesized compound showed a singlet peaks at $\delta=3.92$ and 3.39 ppm attributed to methoxy groups attached to the benzidine rings and multiplet at $\delta=7.95$ – 7.13 ppm due to aromatic protons. The spectrum showed imine proton (CH=N) as a singlet at $\delta=8.59$ ppm. Also, theoretical ^1H NMR calculated chemical shift values of the studied compound were compared to the experimental results in the computational results section. Theoretical ^1H NMR spectrum was given in the Fig 2b.

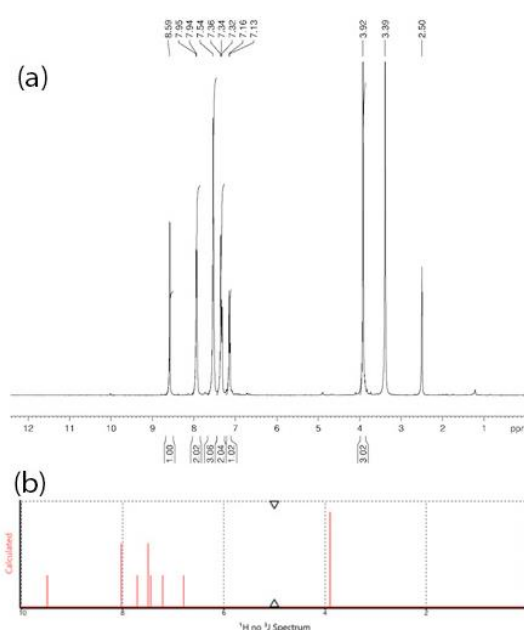


Fig. 2 Comparison of experimental ^1H NMR spectrum of N,N'-Dibenzylidene-3,3'-dimethoxybenzidine (a) and theoretical ^1H NMR spectrum of N,N'-Dibenzylidene-3,3'-dimethoxybenzidine (b).

4.1.3. TGA Analysis

Thermogravimetric analysis was used for investigation of the thermal stability of the title compound and the obtained thermogram is given in Fig. 3. As seen from thermogram, there is a single major weight loss started at 330 °C. The synthesized compound is moisture free and is stable up to 330 °C. The 85% of the compound decomposed at 600 °C. The TGA curves showed that the title compound had high thermal stability (330 °C).

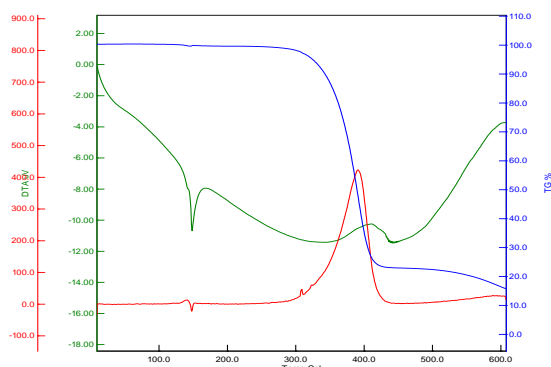


Fig. 3 The TGA curve of the N,N'-Dibenzylidene-3,3'-dimethoxybenzidine.

4.1.4. SEM Analysis

The surface morphology of the title compound was determined using SEM analysis in different magnifications and the SEM micrographs are given in Fig. 4. The SEM micrographs showed that the particles of title compound are agglomerated with different morphologies and in non-uniform size. Also, SEM images of the title compound exhibited irregular shapes.

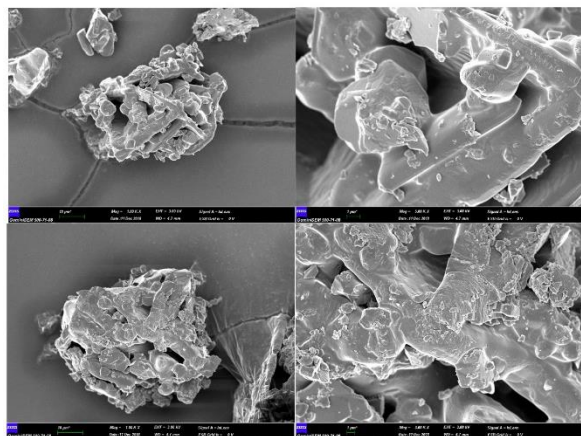


Fig. 4 The SEM micrographs of the title compound with different magnifications.

4.1.5. XRD Analysis

Powder XRD patterns of *o*-dianisidine and N,N'-Dibenzylidene-3,3'-dimethoxybenzidine in the range ($2\theta = 0-50^\circ$) were shown in Fig. 5. XRD pattern of the title compound showed the sharp crystalline peaks indicating its

crystalline solid. As seen from the Fig. 5, XRD pattern of synthesized compound different from the XRD pattern of *o*-dianisidine. Observed peak at 10° for *o*-dianisidine was disappeared in the pattern of N,N'-Dibenzylidene-3,3'-dimethoxybenzidine. Also, the new strongest peaks were observed in the range of 15° and 30° . It can be explained that the change of the crystalline structure is dependent on the formation of a Schiff base. These peaks were observed at Sundararajan et al. study (Sundararajan, 2014).

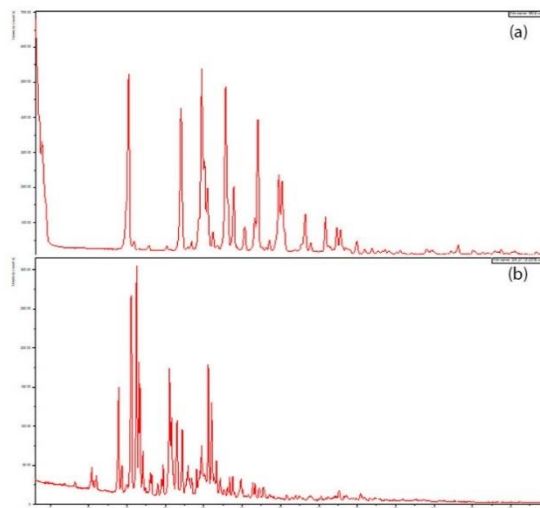


Fig. 5 The XRD patterns of *o*-dianisidine (a) and N,N'-Dibenzylidene-3,3'-dimethoxybenzidine (b)

4.2. Computational results

4.2.1. Geometrical structure

The molecular structure of the synthesized compound was optimized by DFT method. The optimized structure of N,N'-Dibenzylidene-3,3'-dimethoxybenzidine and ORTEP representation along with the labelling of all atoms without H were shown in Fig. 6. The bond lengths, bond angles and dihedral angles of the N,N'-Dibenzylidene-3,3'-dimethoxybenzidine have been provided

by using B3LYP/6-311G** basis set. The calculated values were listed in Table 1.

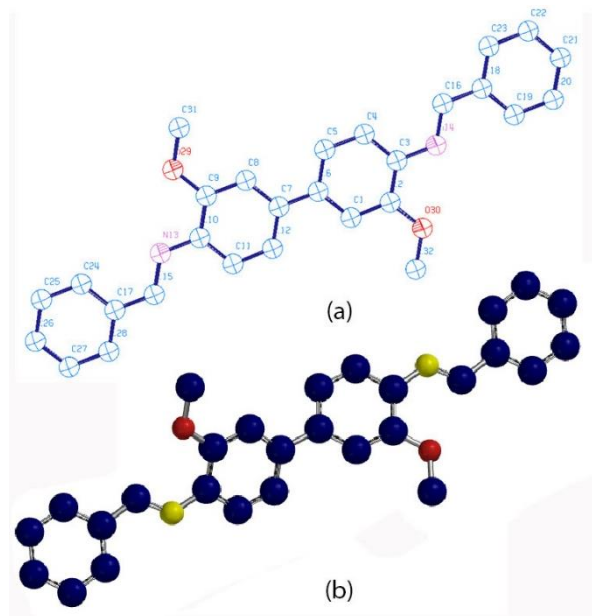


Fig. 6. Ortep 3 diagram and the optimized structure of the N,N'-Dibenzylidene-3,3'-dimethoxybenzidine B3LYP/6-311G** level.

Table 1. Some of the molecular structure parameters of the studied compound computed by using B3LYP/6-311G** level

Parameters		Parameters	
<i>Bond lengths</i> (Å)		<i>Bond angles</i> (°)	
C14-N1	1.281	C15-C14-N1	121.33
N1-C8	1.396	C14-N1-C8	125.17
C11-C10	1.393	N1-C8-C12	115.37
C8-C11	1.423	N1-C8-C11	127.63
C7-C9	1.399	C7-C2-C3	121.53
C10-C7	1.404	C10-C7-C2	120.36
C12-C8	1.402	C7-C2-C1	120.36
C9-C12	1.386	C9-C7-C2	121.53
C2-C3	1.399	C6-C5-N2	127.57
C7-C2	1.481	C5-N2-C13	125.12
C4-C5	1.402	N2-C13-C21	121.33
C3-C4	1.386	C4-C5-N2	115.41
C6-C1	1.393	C13-C21-C24	119.29
C5-C6	1.423	C13-C21-C23	121.84
C1-C2	1.404	<i>Dihedral angles</i> (°)	
C5-N2	1.396	C17-C15-C14-N1	1.25

N2-C13	1.281	C18-C15-C14-N1	-178.75
C13-C21	1.469	C15-C14-N1-C8	-179.67
C21-C24	1.402	C14-N1-C8-C11	22.02
C21-C23	1.404	C14-N1-C8-C13	-160.72
C14-C15	1.469	C10-C7-C2-C3	-39.18
C13-C18	1.402	C9-C7-C2-C1	-39.17
C15-C17	1.404	C9-C7-C2-C3	141.06
C11-O1	1.365	C6-C5-N2-C13	21.89
C6-O2	1.365	C4-C5-N2-C13	-160.89
O2-C28	1.420	C5-N2-C13-C21	-179.60
O1-C27	1.420	N2-C13-C21-C23	0.97
		N2-C13-C21-C24	-179.02

4.2.2. Vibrational Spectra

The DFT/B3LYP method with 6-311G** basis set was used for calculation of vibrational frequencies of N,N'-Dibenzylidene-3,3'-dimethoxybenzidine. In order to explain the correlation between experimental and calculated results, vibrational frequencies obtained from calculations were analysed and compared with the experimental results of the synthesized compound. The results were given in Table 2.

The aromatic symmetric stretching peak of phenyl rings was experimentally observed at 3017.8 cm^{-1} and the theoretically for B3LYP/6-311G** level at 3189 cm^{-1} . The experimental asymmetric and symmetric stretching bands of methoxy groups were recorded at 2962.9 and 2925.8 cm^{-1} respectively, while these peaks were computed at 3078 and 3018 cm^{-1} . Characteristic stretching band of the CH=N group of Schiff bases was recorded at 1626.0

cm⁻¹, that has been calculated at 1631 cm⁻¹ for DFT/B3LYP. The band observed at 1576 cm⁻¹ attributed to the C=C stretching vibrations and it was calculated at 1578 cm⁻¹ for DFT/B3LYP level. The strong absorption bands observed 1247.7 and 1029.9 cm⁻¹ were because of the stretching vibrations of C–O–C and were obtained at 1258 and 1056 cm⁻¹. C–H out-of-plane bending vibrations of phenyl rings were recorded at 848.7, 827.1 and 760.1 cm⁻¹ experimentally and the calculated frequencies corresponded at 849, 830 and 775 cm⁻¹. These results indicated that the experimental and calculated results are in good agreement, statistically ($R^2=0,999$).

4.2.3. NMR Spectra

In order to comparison of the experimental and calculated results, ¹H NMR chemical shift values of N,N'-Dibenzylidene-3,3'-dimethoxybenzidine were computed by using the DFT/B3LYP method with 6-311G** basis set. The experimental and calculated results were given in Table 2.

The spectrum showed that the imine protons (CH=N) were observed as a singlet at δ 8.59 ppm. Theoretical chemical shifts of imine protons were observed at δ 9.49 ppm. Experimentally, ¹H NMR chemical shifts of aromatic rings were recorded at δ 7.13-7.95 ppm. These chemical shifts were calculated at δ 6.79-8.03 ppm. ¹H NMR chemical shifts at 3.39 and 3.92 ppm corresponded to the methoxy substituents of aromatic rings. These signals were computed at 3.90 ppm using the DFT/B3LYP method with 6-311G** basis set. It was found that there is a general correlation between experimental and theoretical NMR studies. It can be concluded that theoretical NMR results can replace with experimental results.

Table 2. The experimental and calculated chemical shifts (ppm) and vibrational frequencies (cm⁻¹) of the title compound.

Frequencies ^a	Experiment al (ppm)	Calculated (B3LYP/6–311G **)
<i>NMR</i>		
H5-H10	8,59	9,49
H13-H12-H11- H17	7,95	8,03
H4-H9	7,32	7,71
H19-H18-H14- H15	7,54	7,50
H20-H16	7,34	7,45
H2-H3	7,16	7,21
H1-H7	7,13	6,79
H8-H22-H23	3,92	3,90
H6-H23-H24	3,39	3,90
		$R^2=0.961$
<i>FT-IR</i>		
	<i>Experiment al (cm⁻¹)</i>	<i>Calculated (B3LYP/6–311G **)</i>
ν (C–H) s of Ph	3017.8	3189
ν (C27–H ₃) as + ν (C28–H ₃) as	2962.9	3078
ν (C27–H ₃) s + ν (C28–H ₃) s	2925.8	3018
ν (C=N) of imine group	1626.0	1631
ν (C=C)	1576.5	1578
α (C27–H ₃) + α (C28–H ₃)	1460.8	1461
ω (C27–H ₃) + ω (C28–H ₃)	1389.8	1406
ν (C–O–C)+ ω (C27–H ₃)+ ω (C28–H ₃)+ γ (C– H) of Ph	1247.7	1258
α (C–H) of Ph + ω (C27–H ₃) + ω (C28–H ₃)	1127.9	1103
ν (C–O)+ γ (C–H) of Ph+ δ (C27–H ₃) + δ (C28–H ₃)	1029.2	1056
ω (C–H) of Ph+ θ of R1+	848.7	849
ω (C–H) of Ph	827.1	840
ω (C–H)	760.1	775
		$R^2=0,999$

^a ν , stretching; α , scissoring; δ , twisting; γ , rocking; θ , ring breathing; ω , wagging; s, symmetric; as, asymmetric.

4.2.4. Atomic charge distributions in gas-phase and solution phase

The Mulliken charges of atoms have an important role in the quantum chemical calculations due to the effect to some properties of compounds, such as vibrational spectra, dipole moment, molecular polarizability Ebrahimi et al. (2013), Tanak, (2011). In order to comparison of the solvent effect for Mulliken charges, the atomic charges distribution of the studied compound were calculated at B3LYP/6-311G** level in gas-phase, polar solvent (DMF) and water. The calculated results were given in Table 3.

As can be seen from Table 3, the N1, N2 atoms of azomethine groups and O1, O2, C27 and C28 atoms of the methoxy groups have bigger negative atomic charges in the gas phase. Also, C1 and C10 atoms of the aromatic rings have relatively more negative charges than the other carbon atoms. On the other hand, H atoms of the methoxy groups have positive charges. At the same time, the negative charges values of the atoms were increased in the solution phase. This means that change of the solvent can change the coordination ability of the discussed atoms. This result may be especially helpful for researcher wanted to use as a ligand to construct metal complexes of this compound.

Table 3. Mulliken atomic charges (e) of the studied compound in gas phase, DMF and water

Atoms	In gas-phase B3LYP/6- 311G**	In solution phase B3LYP/6-311G**	
	($\epsilon=1$)	DMF ($\epsilon=37$)	Water ($\epsilon=78.36$)
H1	+0.226	+0.261	+0.262
C1	-0.312	-0.325	-0.325
C4	-0.208	-0.239	-0.240
C2	+0.015	+0.005	+0.005
C6	+0.287	+0.281	+0.281
C5	+0.116	+0.109	+0.109

C3	-0.205	-0.229	-0.229
H3	+0.194	+0.222	+0.222
H4	+0.200	+0.214	+0.214
C7	+0.015	+0.005	+0.005
C8	+0.117	+0.109	+0.109
C9	-0.204	-0.228	-0.229
C10	-0.312	-0.325	-0.325
C11	+0.28	+0.280	+0.280
C12	-0.207	-0.239	-0.239
H2	+0.194	+0.222	+0.222
H7	+0.226	+0.261	+0.262
H9	+0.200	+0.214	+0.214
N1	-0.355	-0.379	-0.380
N2	-0.355	-0.380	-0.380
C13	-0.027	-0.039	-0.040
H5	+0.202	+0.225	+0.226
C14	-0.026	-0.038	-0.038
H10	+0.20	+0.224	+0.225
C15	-0.011	-0.019	-0.020
C16	-0.181	-0.203	-0.203
C17	-0.161	-0.194	-0.195
C18	-0.209	-0.225	-0.225
C19	-0.196	-0.217	-0.218
C20	-0.193	-0.215	-0.216
H12	+0.206	+0.208	+0.208
H13	+0.191	+0.225	+0.226
H14	+0.193	+0.223	+0.223
H15	+0.195	+0.223	+0.224
H16	+0.194	+0.224	+0.224
C21	-0.011	-0.019	-0.019
C22	-0.181	-0.203	-0.203
C23	-0.161	-0.194	-0.195
C24	-0.209	-0.225	-0.226
C25	-0.196	-0.218	-0.218
C26	-0.193	-0.215	-0.216
H11	+0.206	+0.208	+0.208
H17	+0.191	+0.225	+0.226
H18	+0.193	+0.223	+0.223
H19	+0.195	+0.223	+0.224
H20	+0.194	+0.224	+0.224
O1	-0.358	-0.369	-0.369
O2	-0.359	-0.369	-0.369
C27	-0.463	-0.483	-0.483
H8	+0.218	+0.234	+0.235
H21	+0.230	+0.247	+0.247
H22	+0.213	+0.235	+0.236
C28	-0.463	-0.483	-0.483
H6	+0.218	+0.235	+0.235
H23	+0.230	+0.247	+0.247
H24	+0.213	+0.236	+0.236

4.2.5. Molecular electrostatic potential

Electrophilic and nucleophilic attacks in chemical reactions and hydrogen bonding interactions can be understood with the molecular electrostatic potential surface

(MEP) of the compounds. Also, MEP is a useful parameter to understand the interaction sites of one molecule interacted with another molecule. Especially, it can be explanatory descriptor for interaction between both drug-receptor and enzyme-substrate (Okulik & Jubert, 2005; Scrocco & Tomasi, 1978; Tanak et al. 2019).

The charge distributions of molecules have been illustrated three dimensionally by the electrostatic potential of the molecule created by its nuclei and electrons. Electrostatic potential can be a useful analytical tool to reveal reactive sites of electrostatically dominated noncovalent interactions. It can be determined using by computational methods or by diffraction (Okulik & Jubert, 2005; Politzer, Concha, & Murray, 2000).

In this study, the B3LYP/6-311G** basis set was used for the determination of the MEP. The MEP surface of the N,N'-Dibenzylidene-3,3'-dimethoxybenzidine was given in Fig. 7. As seen from Fig. 6, red and yellow area representing the negative regions were belonged with the electrophilic reactivity. The positive regions showed with blue and green were related to nucleophilic reactivity. The around of the N1 and N2 atoms of the studied molecule observed the negative regions which are possible sites for electrophilic attack. On the other hand, the positive regions showed the possible sites of the nucleophilic attack were localized at H23 and H21 atom of methoxy groups. These results can be concluded that the molecule can have noncovalent interactions with these regions.

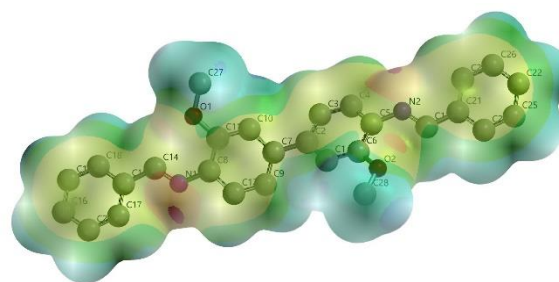


Fig. 7 Molecular electrostatic potential map of the N,N'-Dibenzylidene-3,3'-dimethoxybenzidine calculated by DFT method at B3LYP/6-311G** level.

4.2.6. Frontier molecular orbitals

The highest occupied molecular orbital (HOMO) and lowest unoccupied molecular orbital (LUMO) referred as frontier orbitals play a noteworthy role in the chemical reactions as well as electric and optical properties of molecules (Fleming, 1977; Fukui, 1982). HOMO-1, HOMO, LUMO and LUMO + 1 orbitals were computed using by DFT method at B3LYP/6-311G** basis set and given in the Fig. 8.

As seen from Fig. 8, HOMO-1, HOMO and LUMO were primarily placed on the benzidine ring and azomethine groups. While LUMO+1 was localized on the phenyl rings bonded to the benzidine ring. The energy differences value between with the HOMO and LUMO is a significant parameter for determination of molecular electrical transport properties (Yalçın, Ceylan, Sarıoğlu, Sönmez, & Aygün, 2015). If the molecule has a high frontier orbital gap, it shows low chemical reactivity and high stability (Sinha, Prasad, Narayan, & Shukla, 2011). In the present study, the energy distinction of the HOMO and LUMO is 3,52 eV. This large distinction of the HOMO and LUMO means that the N,N'-Dibenzylidene-3,3'-dimethoxybenzidine has fairly high chemical hardness and kinetic stability.

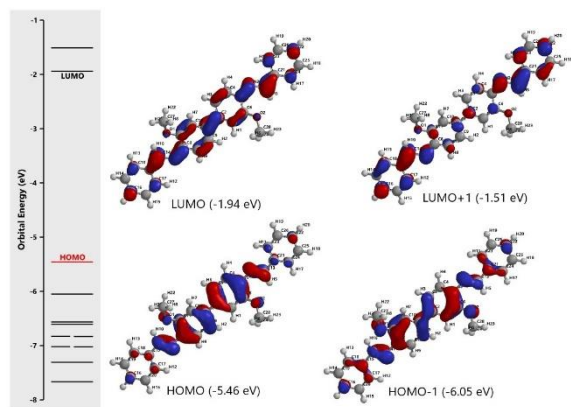


Fig. 8 Molecular orbital surfaces for the HOMO-1, HOMO, LUMO and LUMO+1 of the N,N'-Dibenzylidene-3,3'-dimethoxybenzidine computed at B3LYP/6-311G** level. Energy levels of molecular orbitals were given in parentheses.

4.2.7. Total energies, QSAR parameters and Thermodynamic properties in different solvent media

In order to evaluate the change of total energies, QSAR parameters (Akyüz & Sarıpinar, 2013) and thermodynamic properties of the studied compound in different media, the calculations were performed in two kinds of solvent (DMF and water) and gas phase. Total energies, QSAR parameters, dipole moments and thermodynamic properties have been computed in solvent media and gas phase with DFT method with B3LYP/6-311G** basis set and the results are presented in Table 4.

According to Table 4, it can be determined that polarizability, total energies, ZPE, PSA, volume and area of the studied compound slightly increased with the increase of the solvent polarity. However, the dipole moment and polar area clearly increased with the solvent polarity. The reason for this changes are that the coordination ability of nitrogen and oxygen atoms changes in different solvents.

Table 4. Total energies, QSAR parameters and thermodynamic properties of the N,N'-Dibenzylidene-3,3'-dimethoxybenzidine in different solvents and gas phase

	Gas-phase ($\epsilon=1$)	DMF ($\epsilon=37$)	Water ($\epsilon=78.36$)
<i>QSAR parameters</i>			
Area (\AA^2)	473,05	473,28	473.28
Volume (\AA^3)	456,07	456,65	456.44
PSA (\AA^2)	21,26	21,54	21.54
logP	7,19	7,19	7.19
Polar area (\AA^2)	88,04	182,00	183.19
Polarizability	77,54	77,58	77.56
<i>Thermodynamics</i>			
ZPE (kJ/mol)	1182,55	1184,70	1184.69
H ^o (au)	-	-	-1341.18
	1341,16	1341,19	
S ^o (j/mol.K)	796,93	755,22	757.24
G ^o (au)	-	-	-1341.27
	1341,25	1341,27	
Dipole moment (debye)	1,25	1,30	1.32
Energy (au)	-	-	-1341.66
	1341,64	1341,66	

5. Conclusion

In the present study, N,N'-Dibenzylidene-3,3'-dimethoxybenzidine was synthesized by condensation reaction between o-dianisidine and benzaldehyde and characterized using elemental analysis, FT-IR, H-NMR, TGA, XRD and SEM. Also, the optimized geometrical parameters, spectroscopic properties and physicochemical properties have been computed using the DFT method with B3LYP/6-311G** basis set. The experimental and theoretical results were compared.

FT-IR and ¹H NMR analysis results and the change of the XRD pattern showed that the N,N'-Dibenzylidene-3,3'-dimethoxybenzidine was successfully synthesized. The TGA analysis revealed that the synthesized

compound had high thermal stability (330 °C).

As a consequence of the theoretical calculations, it was found that a well correlation between the experimental and calculated vibrational spectra and ¹H NMR chemical shifts values. Polar area increased with the increasing polarity of the solvent. The N1, N2 atoms of azomethine groups and O1, O2, C27 and C28 atoms of the methoxy groups have bigger negative Mulliken charges in the molecule. Also, the MEP surface of the title compound showed that the around of the N1 and N2 atoms observed the negative regions. The MEP map gave information about that the molecule can have intermolecular interactions and metallic bonding with these regions which are possible sites for electrophilic attack.

Acknowledgement

This work was supported by Aksaray University Research Fund for financial support through Project numbers BAP 2018-025.

6. References

Akyüz, L., & Sarıpınar, E. (2013). Conformation depends on 4D-QSAR analysis using EC-GA method: pharmacophore identification and bioactivity prediction of TIBOs as non-nucleoside reverse transcriptase inhibitors. *Journal of enzyme inhibition and medicinal chemistry*, 28(4), 776-791.

Bachrach, S. M. (2008). *Computational organic chemistry. Annual Reports Section "B"(Organic Chemistry)*, 104, 394-426.

Ebrahimi, H., Hadi, J., & Al-Ansari, H. (2013). A new series of Schiff bases derived from sulfa drugs and indole-3-carboxaldehyde: Synthesis, characterization, spectral and DFT computational studies. *Journal of Molecular Structure*, 1039, 37-45.

Fleming, I. (1977). *Frontier orbitals and organic chemical reactions*: Wiley.

Fukui, K. (1982). The role of frontier orbitals in chemical reactions (Nobel Lecture). *Angewandte Chemie International Edition in English*, 21(11), 801-809.

Gupta, K., Sutar, A. K., & Lin, C.-C. (2009). Polymer-supported Schiff base complexes in oxidation reactions. *Coordination Chemistry Reviews*, 253(13-14), 1926-1946.

Gümrükçü, G., Karaođlan, G. K., Erdođmuş, A., Gül, A., & Avcıata, U. (2012). A novel phthalocyanine conjugated with four salicylideneimino complexes: photophysics and fluorescence quenching studies. *Dyes and Pigments*, 95(2), 280-289.

Im, H., Kim, J., Sim, C., & Kim, T. H. (2018). Crystal structure of N, N'-dibenzyl-3, 3'-dimethoxybenzidine. *Acta Crystallographica Section E: Crystallographic Communications*, 74(3), 271-274.

Karelson, M., Lobanov, V. S., & Katritzky, A. R. (1996). Quantum-chemical descriptors in QSAR/QSPR studies. *Chemical reviews*, 96(3), 1027-1044.

Kaya, I., Yıldırım, M., & Kamacı, M. (2009). Synthesis and characterization of new polyphenols derived from o-dianisidine: the effect of substituent on solubility, thermal stability, and electrical conductivity, optical and electrochemical properties. *European Polymer Journal*, 45(5), 1586-1598.

- Lorcy, D., Bellec, N., Fourmigué, M., & Avarvari, N. (2009). Tetrathiafulvalene-based group XV ligands: Synthesis, coordination chemistry and radical cation salts. *Coordination Chemistry Reviews*, 253(9-10), 1398-1438.
- Okulik, N., & Jubert, A. H. (2005). Theoretical analysis of the reactive sites of non-steroidal anti-inflammatory drugs. *Internet Electronic Journal of Molecular Design*, 4(1), 17-30.
- Politzer, P., Concha, M. C., & Murray, J. S. (2000). Density functional study of dimers of dimethylnitramine. *International Journal of Quantum Chemistry*, 80(2), 184-192.
- Przybylski, P., Huczynski, A., Pyta, K., Brzezinski, B., & Bartl, F. (2009). Biological properties of Schiff bases and azo derivatives of phenols. *Current Organic Chemistry*, 13(2), 124-148.
- Scrocco, E., & Tomasi, J. (1978). Electronic molecular structure, reactivity and intermolecular forces: an euristic interpretation by means of electrostatic molecular potentials *Advances in quantum chemistry* (Vol. 11, pp. 115-193): Elsevier.
- Sinha, L., Prasad, O., Narayan, V., & Shukla, S. R. (2011). Raman, FT-IR spectroscopic analysis and first-order hyperpolarisability of 3-benzoyl-5-chlorouracil by first principles. *Molecular Simulation*, 37(2), 153-163.
- Spartan 18 for Windows, M. a. L. T. a. U. s. G. W., Inc. 2017.
- Sundararajan, M. L., Jeyakumar, T., Anandakumaran, J., & Selvan, B. K. (2014). Synthesis of metal complexes involving Schiff base ligand with methylenedioxy moiety: Spectral, thermal, XRD and antimicrobial studies. *Spectrochimica acta part A: molecular and biomolecular spectroscopy*, 131, 82-93.
- Tanak, H. (2011). DFT computational modeling studies on 4-(2, 3-Dihydroxybenzylideneamino)-3-methyl-1H-1, 2, 4-triazol-5 (4H)-one. *Computational And Theoretical Chemistry*, 967(1), 93-101.
- Tanak, H., Semiz, L., Koçak, F., Açar, A. A., & Özdemir, N. (2019). Molecular structure, spectroscopic and density functional studies on 2-[(5-nitrothiophen-2-yl) methylidene] amino} phenol. *Optik*, 195, 163144.
- Yalçın, Ş. P., Ceylan, Ü., Sarıoğlu, A. O., Sönmez, M., & Aygün, M. (2015). Synthesis, structural, spectral (FT-IR, 1H and 13C NMR and UV-Vis), NBO and first order hyperpolarizability analysis of N-(4-nitrophenyl)-2, 2-dibenzoylacetamide by density functional theory. *Journal of Molecular Structure*, 1098, 400-407.